Thermal and magnetic properties in Ce1-xErxAl2 intermetallic compounds

Thermal and Magnetic Properties in $Ce_{1-x}Er_xAl_2$ Intermetallic Compounds

Masashi Ohashi[1]*, Hidenori Miyagawa[2], Tomohito Nakano[3], Gendo Oomi[2,4], Vladimir Sechovský[5], Isamu Satoh[6], and Takemi Komatsubara[6]

[1]*Faculty of Engineering, Kanazawa University,Kakuma-machi, Kanazawa 920-1192, Japan*
[2]*Department of Physics, Kyushu University, Ropponmatsu, Fukuoka 810-8560, Japan*
[3]*Faculty of Engineering, Niigata University, Niigata 950-2181, Japan*
[4]*Kurume Institute of Technology, Kamitsu-machi, Kurume, Fukuoka 830-0052, Japan*
[5]*Department of Condensed Matter, Charles University, Ke Karlovu 5, 121 16 Prague 2, Czech Republic*
[6] *Institute for Materials Research, Tohoku University, Sendai 980-8577, Japan*

The magnetic and thermal properties of $Ce_{1-x}Er_xAl_2$ compounds have been studied using specific heat, dc magnetization, and ac susceptibility measurements. All these compounds are isomorphic with the $MgCu_2$ Laves phase, and the lattice parameter decreases almost linearly with the increasing Er concentration x. The dc magnetic susceptibility follows the Curie-Weiss law, and the Weiss temperature continuously changes from $\Theta = -24$ K for $x = 0$ to $\Theta = 15$ K for $x = 1$, indicating a change from antiferro-magnetism to ferromagnetism. Θ changes from negative to positive at around $x = 0.2$ where where a field-induced meta-magnetic transition disappears. The magnetic ordering state continuously changes with the change in x from antiferromagnetc to ferromagnetic through a spin-glass-like behavior.

KEYWORDS: spin glass, heat capacity, susceptibility, $CeAl_2$, $ErAl_2$

1. Introduction

The magnetic properties of intermetallic compounds containing rare-earth elements have been an object of great interest.[1–3] The binary compounds of RAl_2 (R: rare earth) are the prototypes of rare-earth compounds with non magnetic metals, and show a wide range of electronic and magnetic properties by changing R. Many RAl_2 compounds melt congruently, so it is easy to grow them even in the form of single crystals. The crystal structure is relatively simple: isomorphic $MgCu_2$ type with the space group $Fd\bar{3}m$ (C15 Laves phase).[4] The interest

*E-mail: ohashi@se.kanazawa-u.ac.jp

in them is enhanced by the fact that compounds in which $4f$ electrons are localized are often model systems in which quantitative analysis can be performed, allowing for an accurate determination of the relevant interactions. Almost all RAl_2 compounds show ferromagnetic ordering with different Curie temperatures T_C.[5,6] It is well known that the exchange coupling between the localized $4f$-electron shells of rare-earth ions is due to the conduction electrons and is called the Ruderman-Kittel-Kasuya-Yoshida (RKKY) interaction.

On the other hand, $CeAl_2$ is a special case among the RAl_2 compounds. Since the f-level of $CeAl_2$ is energetically close to the conduction-electron band, both magnetic and hybridization interactions between f levels and the conduction-electron band are vital for the determination of the ground state. Considerable attention has been focused on $CeAl_2$ as a system that shows the competition between these magnetic and nonmagnetic interactions. An antiferromagnetic ordering due to a spin density wave occurs at T_N = 3.8 K,[7–9] whereas Kondo-type conduction-electron screening of the localized moments occurs above T_N, which is suppressed by applying pressure since T_N is merged to the Kondo temperature T_K.[8] Below T_N, a pronounced jump in the magnetization has been observed at a magnetic field of approximately 5 T in a $CeAl_2$ single crystal. It indicates a metamagnetic phase transition from the antiferromagnetic ordering phase to the paramagnetic ordering phase.[10] At higher magnetic phases, the magnetization curve along the easy axis [111] is the highest.

Therefore, the substitution of Ce by another rare-earth element R causes changes in the magnetic interaction. If we choose R such that RAl_2 shows a ferromagnetic transition, interesting magnetic properties are expected to be observed in the pseudobinary system $Ce_{1-x}R_xAl_2$ because of the competition between the ferromagnetic interaction of RAl_2 (x = 1) and the antiferromagnetic interaction of $CeAl_2$ (x = 0). In particular, $ErAl_2$ exhibits ferromagnetic ordering at approximately T_C =13 K,[11] which is relatively close to the T_N of $CeAl_2$ compared with the T_C of the other RAl_2 compounds. Moreover, the easy axis of $ErAl_2$ is [111],[12,13] which is the same as that of $CeAl_2$ in the antiferromagnetic ground state. These findings indicate that it is relatively easy to tune the ground state of the pseudobinary system $Ce_{1-x}Er_xAl_2$ by changing the amounts of Er and Ce.

In this paper, we present the crystallography, magnetization, and specific heat of $Ce_{1-x}Er_xAl_2$ with $0 < x < 1$. We also describe the influence of Er substitution on the magnetic properties of the $Ce_{1-x}Er_xAl_2$ system, which presents a complex magnetic phase diagram with antiferromagnetism, ferromagnetism, and spin-glass states.

2. Experimental Methods

Single crystals of $Ce_{1-x}Er_xAl_2$ were grown by the Czochralski pulling method from a melt of stoichiometric amounts of the constituent elements in a tetra-arc furnace. All ingots were confirmed to be single crystals from their Laue patterns. The crystal structure and lattice parameter were determined using X-ray powder diffraction analysis. The dc magnetization was measured in a magnetic field with the easy axis [111], using the Quantum-Design MPMS. The ac magnetic susceptibility was measured at a modulation field along [111] using the Quantum-Design PPMS. The specific heat was measured by thermal relaxation using the Quantum-Design PPMS.

3. Results and Discussion

The crystal structures of the pseudobinary alloy system $Ce_{1-x}Er_xAl_2$ are confirmed to be of the cubic C15 Laves phase. The lattice parameters a of $CeAl_2$ and $ErAl_2$ are 8.066 and 7.791 Å, respectively, which are comparable with those in a previous report.[4)] For $Ce_{1-x}Er_xAl_2$, a decreases with increasing x, which is due to the lanthanoid contraction. Figure 1 shows the cell volume variation of $Ce_{1-x}Er_xAl_2$ as a function of the Er concentration x. A linear Vegard law is obtained without significant changes in volume.

Figure 2 shows the temperature dependence of the specific heat $C(T)$ of the samples with different x. For $CeAl_2$, an anomaly occurs at T_N= 3.8 K owing the antiferromagnetic phase transition. Above T_N, the coefficient of the linear term in the specific heat is calculated to be γ = 112 mJ/mol·K^2, which is comparable to the previously reported value of γ = 135 mJ/mol·K^2.[14)] The inset of Fig. 2 shows the detailed behavior at temperatures below 6 K. With increasing x, the sharp peak becomes broad, and the temperature at which the peak is observed decreases with increasing Er concentration. For $x = 0.4$, there is no peak in $C(T)$, indicating that the antiferromagnetic ordering is suppressed. On the other hand, a peak appears again on the $C(T)$ curve of $x = 0.6$ at approximately 6.6 K. As the amount of Er substitution increases from $x = 0.6$, the peak becomes sharper. The temperature of the peak increases and is determined to be 12.5 K for $ErAl_2$ (x=1), which is consistent with the ferromagnetic transition temperature T_C= 13 K.[11)]

Figure 3 shows the magnetic field dependence of the magnetization $M(B)$ of $Ce_{1-x}Er_xAl_2$ at 2 K. For $x = 0$, $M(B)$ increases linearly with increasing magnetic field up to 5 T. The metamagnetic transition due to the collapse of antiferromagnetism is observed at $B_M \sim 4.6$ T. To clarify this anomaly, the first derivative of $M(B)$, dM/dB, was calculated at 2 K. As shown in the inset of Fig. 3, B_M corresponds to the magnetic field exhibiting the peak. With

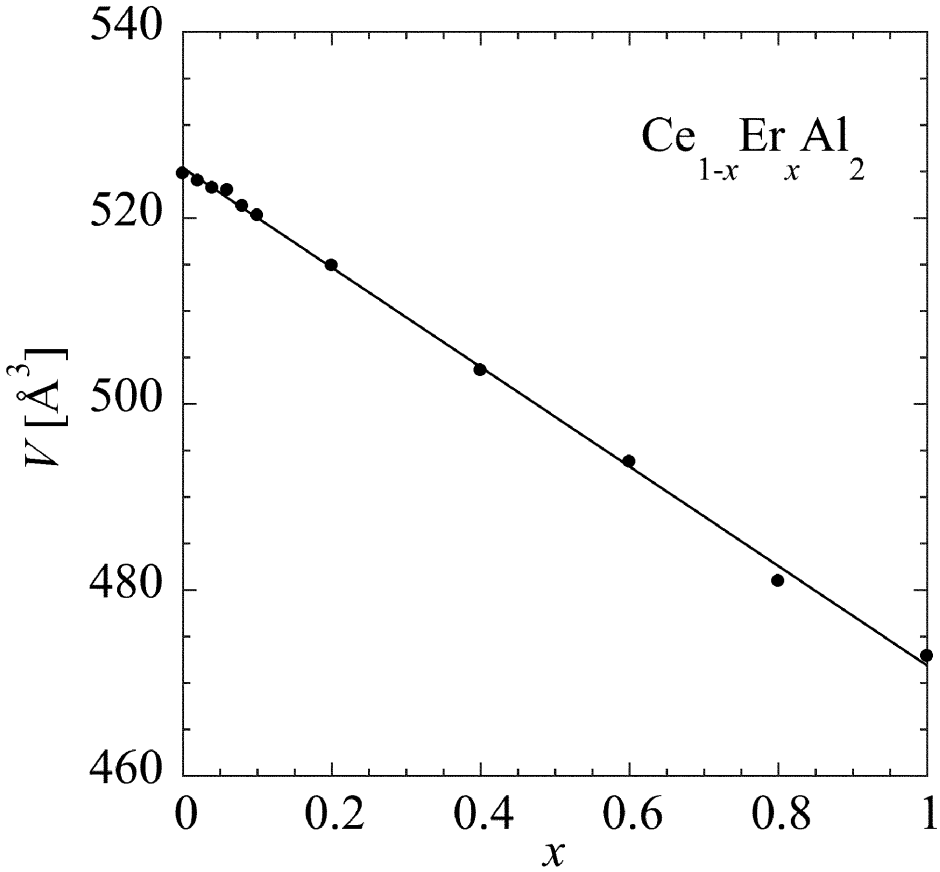

Fig. 1. Concentration x dependence on the cell volume $V = a^3$ in $Ce_{1-x}Er_xAl_2$. The solid line is the least-squares fit of the function $V = 525.4 - 53.5 \times x$ (Å^3).

increasing the amount of Er substitution, the anomaly becomes broad, and B_M is suppressed. This will be discussed later.

The magnetization of $Ce_{1-x}Er_xAl_2$ increases with increasing x, since the localized magnetic moment of Er^{3+} is larger than that of Ce^{3+}. For $x = 1$, the ferromagnetic behavior with hysteresis is observed at 2 K, which was not observed in previous studies. The magnetization at 7 T in $ErAl_2$ is 7.7 μ_B/Er^{3+}, which is in good agreement with previous reports.[12,13)]

Figure 4 shows the temperature dependence of the inverse susceptibility $\chi^{-1}(T)$ of $Ce_{1-x}Er_xAl_2$. In all compounds, $\chi^{-1}(T)$ follows the Curie-Weiss law above 50 K. For x=0, the effective magnetic moment μ_{eff} and the Weiss temperature Θ_W are observed to be 2.3μ_B and −24 K, respectively. μ_{eff} is close to that of the Bohr magneton of Ce^{3+}, $\mu_{Ce^{3+}} = 2.54\mu_B$. As x increases, both μ_{eff} and Θ_W increase. For $x = 1$, μ_{eff} and Θ_W are observed to be 9.7μ_B and 15 K, respectively. μ_{eff} is close to that of the Bohr magneton of Er^{3+}, $\mu_{Er^{3+}} = 9.59\mu_B$.

The x dependences of the metamagnetic transition field (B_M), effective Bohr magneton

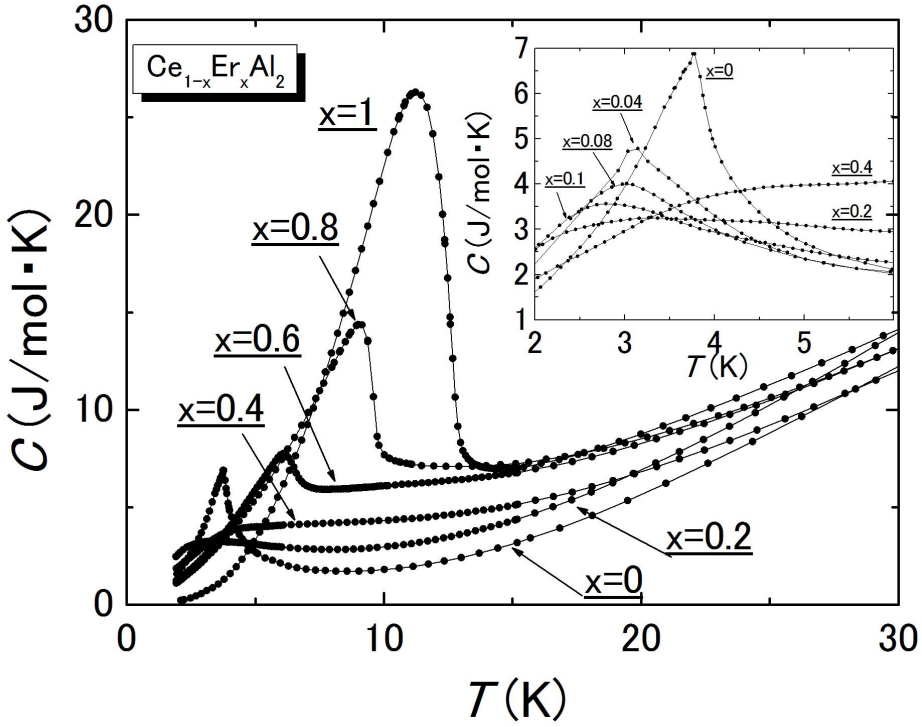

Fig. 2. Temperature dependence of magnetic specific heat in $Ce_{1-x}Er_xAl_2$. The inset shows the extended figure at low temperature.

number ($\mu_{\rm eff}$), and paramagnetic Curie temperature ($\Theta_{\rm W}$) are shown in Figs. 5 (a), 5 (b), and 5 (c), respectively. The $B_{\rm M}$ of $Ce_{1-x}Er_xAl_2$ decreases linearly from $B_{\rm M}$ = 4.6 T for $x = 0$ as Er concentration increases. It appears that $B_{\rm M}$ disappears at $x \sim 0.1$. $\mu_{\rm eff}$ is described by the function

$$\mu_{\rm eff} = (\mu^2_{\rm Ce^{3+}} \times (1-x) + \mu^2_{\rm Er^{3+}} \times x)^{\frac{1}{2}} (\mu_{\rm B}/{\rm atom}), \tag{1}$$

which is shown as the solid line in Fig. 5 (b). It indicates that the magnetic moment comes from the average of the magnetic moments of the rare earth elements in the $Ce_{1-x}Er_xAl_2$ ion in the paramagnetic region. As shown in Fig. 5 (c), $\Theta_{\rm W}$ also increases with x. The negative $\Theta_{\rm W}$ for $x < 0.2$ is consistent with the existence of the antiferromagnetic ground state in $CeAl_2$. We find that the sign of $\Theta_{\rm W}$ changes from negative to positive at around x= 0.2, indicating that the antiferromagnetism of $CeAl_2$ changes to ferromagnetism by substituting Er for Ce.

To investigate the magnetic ordering state in detail, we performed ac susceptibility measurements for several frequencies. Figure 6 shows the temperature dependence on the real component $\chi'(T)$ of ac susceptibility for a frequency of 100 Hz. All $\chi'(T)$ curves of the $Ce_{1-x}Er_xAl_2$ compounds show similar behaviors, and have a single maximum. Here, we de-

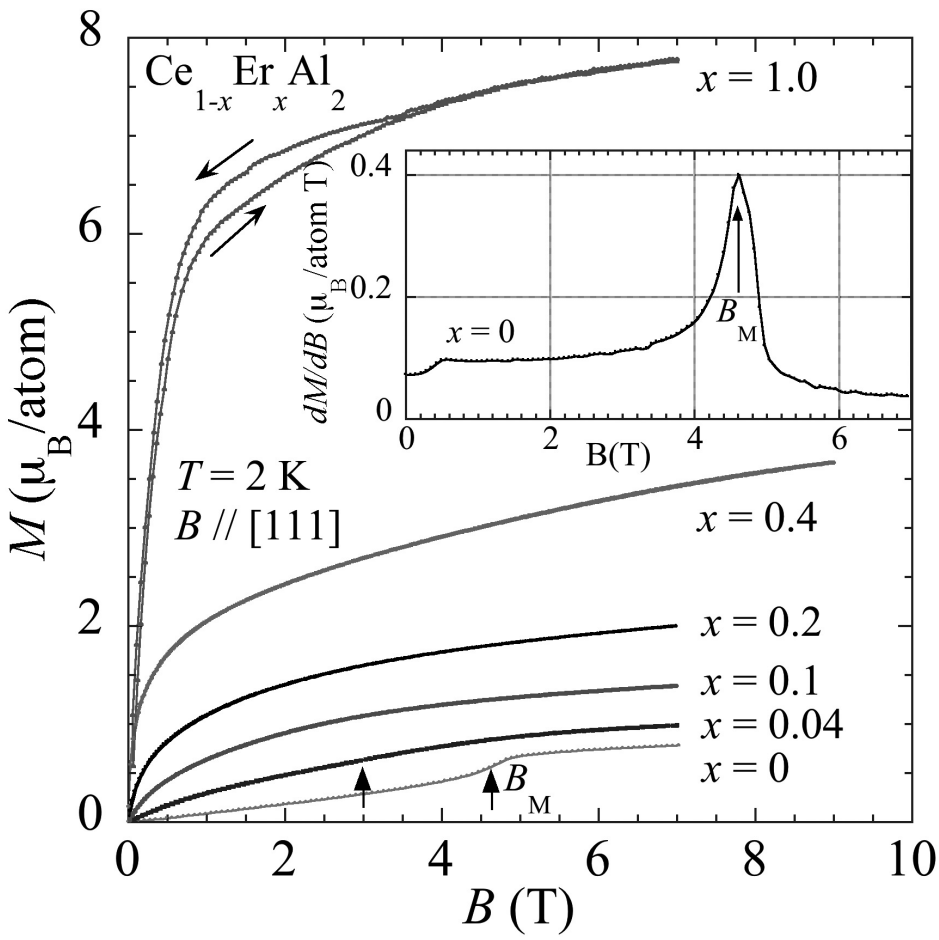

Fig. 3. Magnetic field dependence of magnetization at 2 K in $Ce_{1-x}Er_xAl_2$. Inset: the magnetic field dependence of first derivative of $M(B)$ at 2 K in $CeAl_2$. The magnetic field was applied along the easy axis [111].

fine T_M as the temperature where the $\chi'(T)$ curve shows a maximum. For $CeAl_2$ ($x = 0$), a peak is clearly visible at $T_M \sim 3.8$ K, which corresponds to the antiferromagnetic transition temperature observed in the heat capacity in Fig 2. Although T_M decreases as Er concentration x increases from 0 to 0.2, it increases for $x > 0.2$ where antiferromagnetism ordering disappears.

It is found that a $\chi'(T)$ exhibits a significant frequency-dependent shift of T_M for several compounds. Figure 7 shows a typical example of the $\chi'(T)$ curve for $Ce_{0.9}Er_{0.1}Al_2$ below 4.0 K for several frequencies. All the $\chi'(T)$ curves exhibit pronounced maxima, and both amplitude and position depend on the frequency of the applied magnetic field, particularly in the low-frequency range. This result indicates the formation of a spin-glass state in $Ce_{0.9}Er_{0.1}Al_2$ with a spin freezing temperature of $T_M = 2.56$ K (at a frequency of $f = 100$ Hz) determined from the peak position of $\chi'(T)$.

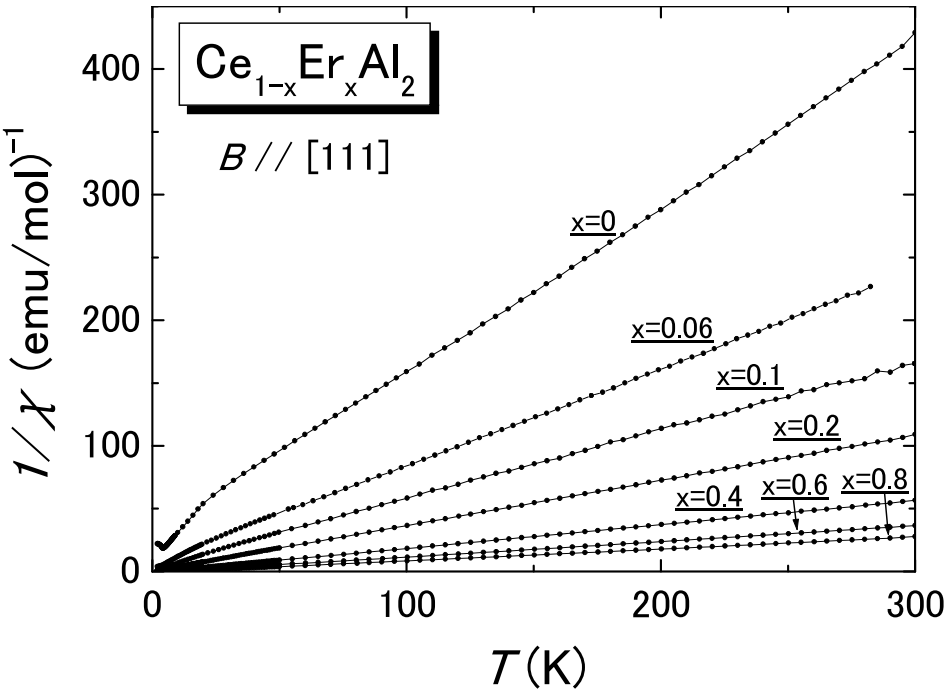

Fig. 4. Temperature dependence of the inverse magnetic susceptibility in $Ce_{1-x}Er_xAl_2$.

Here, we inspected the spin dynamics by applying a simple formula, which corresponds to the shift of the ac-susceptibility maxima per frequency decade,

$$\delta T_{\mathrm{M}} = \frac{\Delta T_{\mathrm{M}}}{T_{\mathrm{M}} \Delta \log f}. \tag{2}$$

The obtained δT_{M}'s are 0.0047, 0.021, and 0.042 for $x = 0.08$, 0.1, and 0.2, respectively. These values are comparable to those reported for other metallic spin-glass systems, e.g., CuMn: 0.005,[15] AuFe: 0.010,[15] U_2RhSi_3: 0.008,[16] URh_2Ge_2,[17] $PrNi_{1-x}Cu_xAl$: 0.006 - 0.012,[18] and Nd_2AgIn_3: 0.015.[19] To investigate the nature of the spin-glass state in greater detail, the well-known Vögel-Fulcher law[20] was applied to the data as follows:

$$f = f_0 \exp \frac{-E_a}{k_B(T_{\mathrm{M}} - T_0)}, \tag{3}$$

where f is the applied frequency, f_0 is the characteristic frequency, E_a is the activation energy, which determines the energetic barrier for spins to align with the external magnetic field, T_0 is the Vögel-Fulcher temperature, which corresponds to the interspin or intercluster interaction, and k_B is the Boltzmann constant. We tested various f_0 values near the characteristic value of 10^{13} Hz, which is typical for a spin-glass system.[21] Although the activation energies change upon varying f_0, they still lie in reasonable ranges when considering the freezing temperatures. Figure 8 shows the fit of freezing temperatures using Eq. (3) for the $Ce_{1-x}Er_xAl_2$ series of $x = 0.08$, 0.1, and 0.2, where the f_0 parameter is fixed at 10^{13} Hz. The

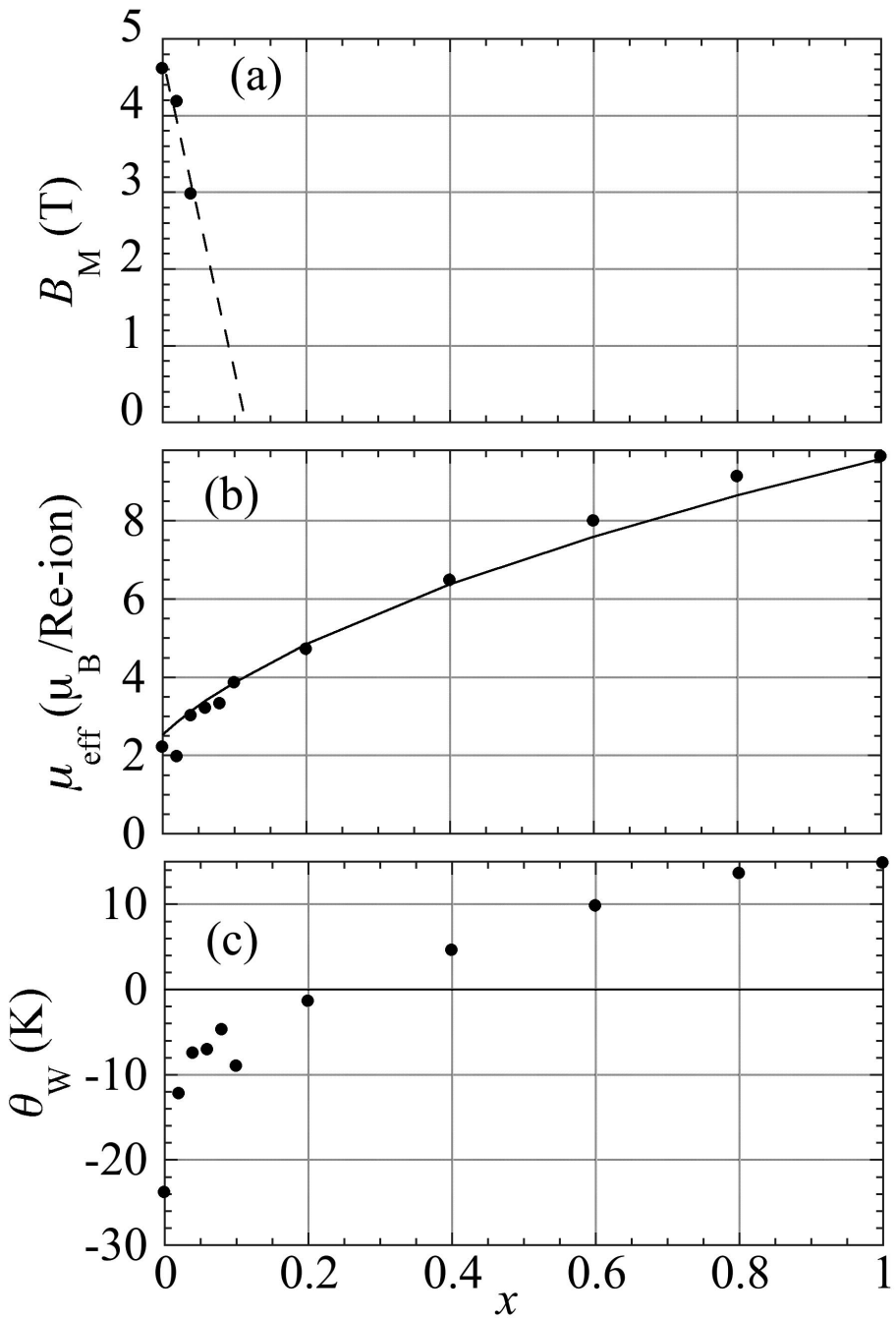

Fig. 5. (a) Metamagnetic transition field B_M, (b) Bohr magneton μ_{eff}, and (c) Weiss temperature Θ_W vs Er concentration in $Ce_{1-x}Er_xAl_2$.

slope gives the activation energy E_a. The intercept with the y-axis corresponds to T_0. The obtained parameters are summarized in Table I. In general, the activation energies E_a are one order higher than the values of T_0 for compounds that show the spin-glass-like behavior. In the case of $Ce_{1-x}Er_xAl_2$, the data between x=0.1 and 0.4 provide evidence of the formation of a collective spin-glass-like state.

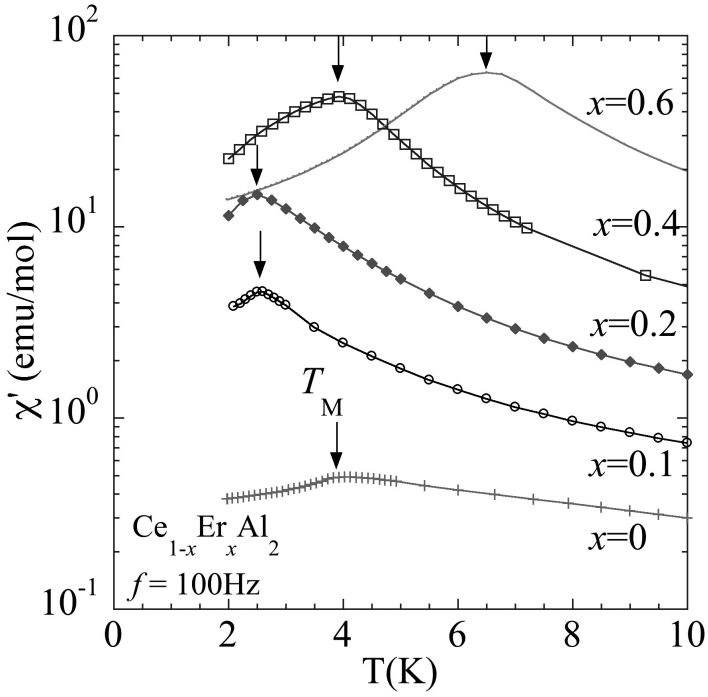

Fig. 6. Temperature dependence of ac susceptibility χ' at 100 Hz for $Ce_{1-x}Er_xAl_2$.

Table I. Values of parameters obtained from fitting of freezing temperatures using the Vögel-Fulcher law for $Ce_{1-x}Er_xAl_2$ compounds and several spin-glass systems.

	E_a/k_B (K)	T_0 (K)
$Ce_{0.96}Er_{0.04}Al_2$	0	3.18
$Ce_{0.92}Er_{0.08}Al_2$	3.33	2.60
$Ce_{0.9}Er_{0.1}Al_2$	14.3	2.00
$Ce_{0.8}Er_{0.2}Al_2$	28.8	1.36
$Ce_{0.6}Er_{0.4}Al_2$	13.1	3.42
$Ce_{0.4}Er_{0.6}Al_2$	5.42	6.32
$PdMn_{8\%}$ [15]	39	3.6
$AuFe_{10\%}$ [15]	81	29.1
$La_{1-x}Gd_xAl_2$ [15]	4.6	0
$PrNi_{0.5}Cu_{0.5}Al$ [18]	28.8	3.0
Nd_2AgIn_3 [19]	111.4	9.7

Finally, considering the present data, the magnetic phase diagram of $Ce_{1-x}Er_xAl_2$ is compiled in Figure 9. In general, the magnetic susceptibility of Kondo compounds increases with decreasing temperature, reaches a maximum, and then decreases to a modestly large value at T = 0.[22] This general temperature dependence is described well by a Bethe Ansatz solu-

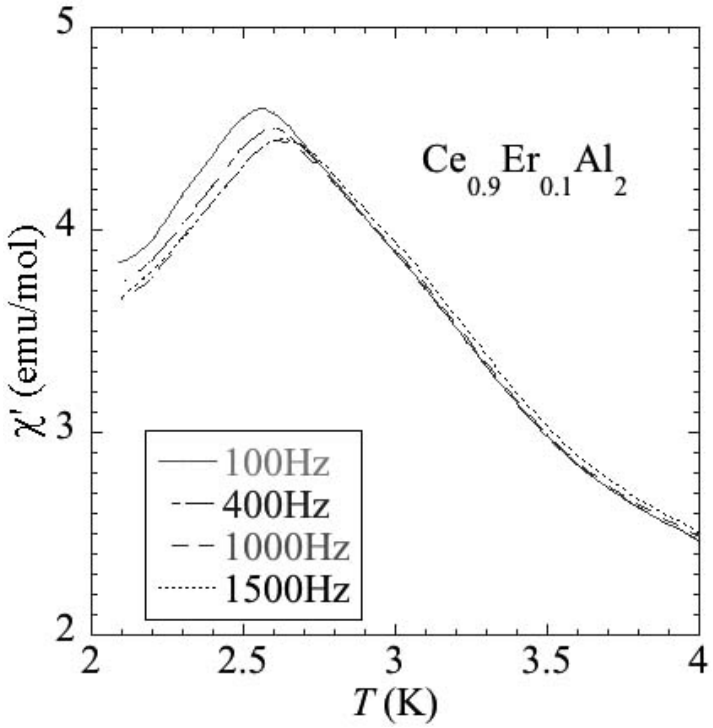

Fig. 7. Temperature dependence of ac susceptibility $\chi'(T)$ of $Ce_{0.9}Er_{0.1}Al_2$ for several frequencies.

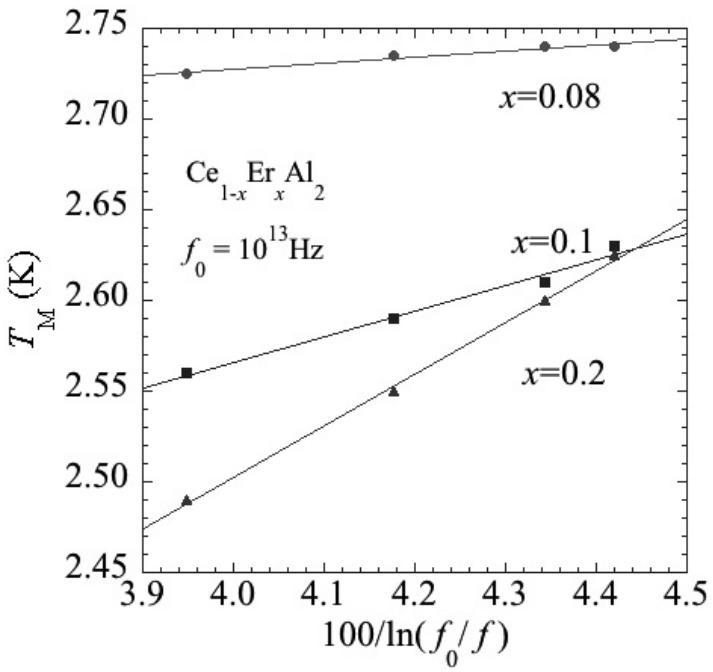

Fig. 8. Plots of T_M vs $100/\ln(f_0/f)$ for the $Ce_{1-x}Er_xAl_2$ series of x = 0.08, 0.1, and 0.2. The solid line is the least-squares fit using Eq. (3). f_0 was fixed at 10^{13} Hz. The obtained parameters are summarized in Table I.

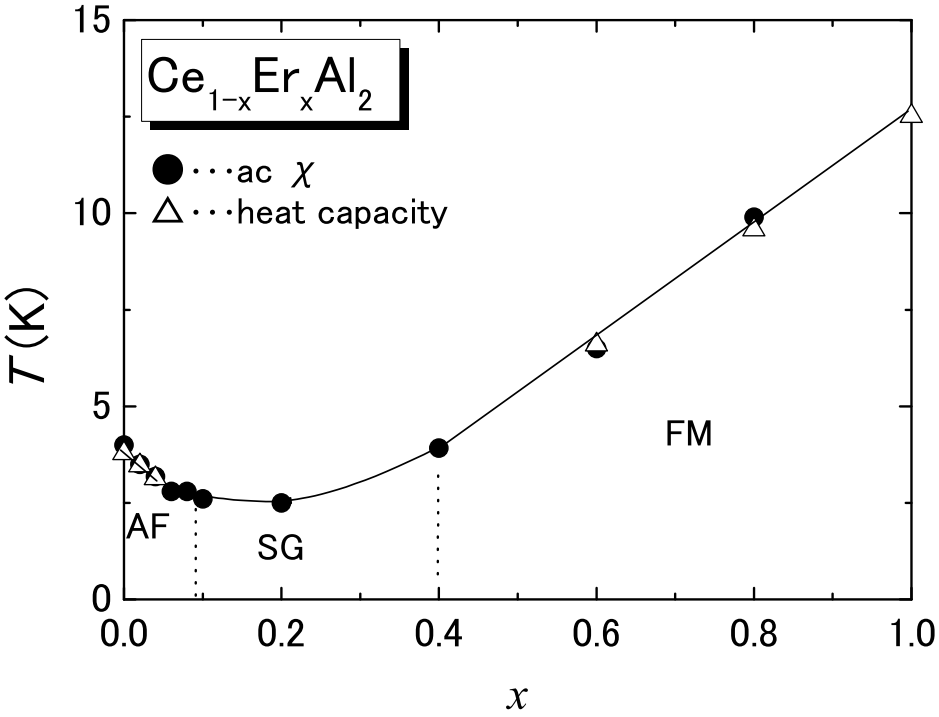

Fig. 9. Schematic phase diagram of $Ce_{1-x}Er_xAl_2$ systems.

tion of the Coqblin-Schrieffer model of Kondo impurities.[23,24] This theory predicts a single-impurity Kondo temperature T_K of approximately $3T_M$ for Ce compounds. However, in the case of $CeAl_2$ ($x = 0$), T_M can be influenced not only by the Kondo effect but also by antiferromagnetic interactions, since T_K is close to $T_N = 3.8$ K.[8] T_M decreases as Er concentration increases from $x = 0$. Since the coefficient dT_M/dx approaches dT_N/dx, which is estimated from the sharp peak of the temperature dependence of the specific heat. This means that the x dependence on T_M corresponds to that on T_N, at least up to x of approximately 0.08.

The $T_M - x$ curve shows a minimum at around $x = 0.2$. As discussed before, a spin-glass-like-behavior appears between $x = 0.1$ and 0.4, where the values of E_a are one order higher than that of T_0. It seems that T_M corresponds to the freezing temperature from the paramagnetic state to the spin-glass state. For $x > 0.6$, on the other hand, the spin-glass-like behavior disappears when E_a is smaller that T_0. In this region, T_M increases with increasing x and is close to the Curie temperature T_C obtained from the results of the specific heat measurement. This result indicates that the ferromagnetic state is stable and that T_M corresponds to T_C for $x > 0.6$.

4. Summary

In this work, we performed specific heat, dc magnetization, and ac susceptibility measurements on single crystals of $Ce_{1-x}Er_xAl_2$. The magnetic behavior upon changing from an antiferromagnetic ($CeAl_2$) ground state to a ferromagnetic ($ErAl_2$) ground state was determined. The magnetic ordering temperature changed continuously as a function of Er concentration x. Spin glass like behavior was observed at around $x = 0.1 - 0.4$.

Acknowledgments

This work was supported in part by grants from The Asahi Glass Foundation, JFE 21st century Foundation, the Japan Securities Scholarship Foundation, The Kyoto Technoscience Center Foundation, and JGC-S Scholarship Foundation.

References

1) Y. Uwatoko, I. Umehara, M. Ohashi, T. Nakano and G. Oomi: *Handbook on the Physics and Chemistry of Rare Earths, Chap. 252*, ed. by K. A. Gschneidner Jr. and L. Eyring (North-Holland Amsterdam, 2012) p. 1.

2) M. Ohashi, G. Oomi, S. Koiwai, M. Hedo, and Y. Uwatoko: Phys. Rev. B **68** (2003) 144428.

3) M. Ohashi, G. Oomi, and I. Satoh: J. Phys. Soc. Jpn. **76** (2007) 114712.

4) A. Iandelli and A. Palenzona: *Handbook on the Physics and Chemistry of Rare Earths, Chap. 13*, ed. by K. A. Gschneidner Jr. and L. Eyring (North-Holland Amsterdam, 1979) p. 1.

5) H. R. Kirchmayr, C. A. Poldy, W. Steiner and G. Wiesinger: *Handbook on the Physics and Chemistry of Rare Earths, Chap. 14*, ed. by K. A. Gschneidner Jr. and L. Eyring (North-Holland Amsterdam, 1979) p. 55.

6) T. Oishi, M. Ohashi, H. Suzuki, and I. Satoh: Journal of Physics: Conference Series **200** (2010) 082022.

7) B. Barbara, M. F. Rossignol, J. X. Boucherle and C. Vettier: Phys. Rev. Lett. **45** (1980) 938.

8) H. Miyagawa, G. Oomi, M. Ohashi, I. Satoh, T. Komatsubara, M. Hedo and Y. Uwatoko: Phys. Rev. B **78** (2008) 064403.

9) S. Tomisawa, S. Wada, M. Ohashi and G. Oomi, J. Phys.: Condens Matter, **18** (2006) 10413.

10) B. Barbara, M. F. Rossignol, J. X. Boucherle, J. Schweizer and J. L. Buevoz: J. Appl. Phys., **50** (1979) 2300.

11) J. C. P. Campoy, E. J. R. Plaza, A. A. Coelho, and S. Gama: Phys. Rev. B **74** (2006) 134410.

12) H. G. Purwins: Physics Letters **31A** (1970) 523.

13) H. Oesterreicher and W. E. Wallace: J. Less-Commom Metals **13** (1967) 91.

14) F. Steglich, C. D. Bredl, M. Loewenhaupt, and K. D. Schotte: J. de Phys. Coll. **C5** (1979) 301.

15) J. A. Mydosh: *Spin Glass: An Experimental Introduction* (Taylor & Francis, London 1993).

16) D. X. Li, A. Dönni, Y. Kimura, Y. Shiokawa, Y. Homma, Y. Haga, E. Yamamoto, T. Honma and Y. Onuki: J. Phys.: Conens. Matter **11** (1999) 8263.

17) S. Süllow, G. J. Nieuenhuys, A. A. Menovsky, J. A. Mydosh, S. A. M. Mentink, T. E. Mason and W. J. L. Buyers: Phys. Rev. Lett. **78** (1997) 354.

18) J. Fikacek, P. Javorsky, J. Vejpravova, J. Prchal, J. Kastil, G. Nenert and E. Santava: Phys. Rev. B **85** (2012) 214410.

19) D. X. Li, S. Nimori, Y. Shiokawa, A. Tobo, H. Onodera, Y. Haga, E. Yamamoto and Y. Onuki, Appl: Phys. Lett. **79** (2001) 4183.

20) G. S. Fulcher: J. Am. Ceram. Soc **8** (1925) 339.

21) J. L.Tholence, Solid State Commun.: **35** (1980) 113.

22) S. A. Shaheen, J. S. Schilling, S. H. Liu and O. D. McMasters: Phys. Rev. B **27** (1983) 4325.

23) V. T. Rajan: Phys. Rev. Lett. **51** (1983) 308.

24) P. Schlottmann: Phys. Rep. **181** (1989) 1.